JOURNAL OF ENERGY SYSTEMS

2024, 8(2)

2602-2052 DOI: 10.30521/jes.1283526 Research Article

Research of hydrodynamic processes in the flow part of a low-flow thermopressor

Dmytro Konovalov
Admiral Makarov National University of Shipbuilding, Thermal Engineering Department, Mykolayiv, Ukraine, dimitriyko79@gmail.com

Halina Kobalava
Admiral Makarov National University of Shipbuilding, Thermal Engineering Department, Mykolayiv, Ukraine, g.lavamay@gmail.com

Roman Radchenko
Admiral Makarov National University of Shipbuilding, Turbines Department, Mykolayiv, Ukraine, ronirad19@gmail.com

Mykola Radchenko *
Admiral Makarov National University of Shipbuilding, Conditioning and Refrigeration Department, Mykolayiv, Ukraine, nirad50@gmail.com

Anatoliy Zubarev
Admiral Makarov National University of Shipbuilding, Conditioning and Refrigeration Department, Mykolayiv, Ukraine, anatoly.zubarev@nuos.edu.ua

Felix Tsaran
Admiral Makarov National University of Shipbuilding, Conditioning and Refrigeration Department, Mykolayiv, Ukraine, felseras@gmail.com

Artem Hrych
Admiral Makarov National University of Shipbuilding, Conditioning and Refrigeration Department, Mykolayiv, Ukraine, artem.grich@gmail.com

Sergey Anastasenko
Admiral Makarov National University of Shipbuilding, Pervomaysk Scientific and Educational Institute, Mykolayiv, Ukraine, ondi2008@ukr.net

Submitted: 14.05.2023
Accepted: 07.03.2024
Published: 30.06.2024

* *Corresponding Author*

Abstract: This research explores the hydrodynamic processes within the flow section of a low-flow thermopressor as a jet-type heat exchanger that utilizes the instantaneous evaporation of highly dispersed liquid in accelerated superheated gas flow resulting in reducing gas temperature with minimum resistance losses in contrast to conventional surface heat exchanger. The efficiency of thermopressor, as a contact heat exchanger, is highly dependent on the design of the flow section and the water injection nozzle. Geometric characteristics perform a crucial role in shaping gas-dynamic processes along the length of the thermopressor's flow section, influenced by resistance losses and local resistance in the tapering and expanding channel segments. Therefore, the optimum thermopressor design has to ensure minimize pressure losses. Using Computational Fluid Dynamics (CFD), the prototype thermopressor models were simulated and the results were compared with experimental data. The empirical equations for local resistance coefficients of thermopressor diffuser and confuser were received to evaluate the impact of various design parameters. The obtained local resistance coefficients for the confuser ranged from 0.02 to 0.08 and for the diffuser – from 0.08 to 0.32. The practical recommendations on geometric and operating parameters and characteristics for enhancing the efficiency of hydrodynamic processes in thermopressor flow part were given.

Keywords: *Confuser, Diffuser, Local resistance coefficient*

Cite this paper as: Konovalov, D., Kobalava, H., Radchenko, R., Radchenko, M., Zubarev A., Tsaran, F., Hrych, A., & Anastasenko S. Research of hydrodynamic processes in the flow part of a low-flow thermopressor. *Journal of Energy Systems 2024; 8*(2): 89-100, DOI: 10.30521/jes.1283526

© 2024 Published by peer-reviewed open access scientific journal, JES at DergiPark (https://dergipark.org.tr/jes)

1. INTRODUCTION

The application of a two-phase jet apparatus, particularly the thermopressor, is a promising method for cooling the working fluid in power plants based on gas turbines and internal combustion engines. One of the promising research areas in modern jet technologies pertains to the study of gas-dynamic processes in thermopressors. A thermopressor is a jet-type contact heat exchanger desired for efficient cooling gas even with small pressure increase achieved through the instantaneous evaporation of highly dispersed liquid injected into accelerated gas flow with minimum surface friction. The design factors significantly influence the working processes of the thermopressor.

The thermopressor effectiveness depends on the total pressure losses due to the following factors: Surface and internal friction of the air, aerodynamic resistance of the injection system, resistance of the injected liquid, processes of heat and mass transfer. Such losses can be quite significant and amount to 10–40%, depending on the design features of the apparatus flow part. Therefore, the development of designing methodology is aimed to determine the geometry of the thermopressor flow part to provide efficient hydrodynamic processes with minimum pressure losses ensuring their effective implementation into power plant work processes. Consequently, it is important to develop the methodology for precise calculating the pressure losses including the diffuser and confuser resistance.

2. LITERATURE REVIEW

A general way to increase the efficiency of power plants is to utilize the exhaust heat [1–3] and cool the working fluid [4] to provide favorable conditions for their efficient operation by application of waste heat recovery chillers [5,6] or electrically driven vapor compression refrigeration machines as in air conditioning system [7,8]. The air is a general working fluid in the majority of the power plants based on combustion engines, in particular, gas turbines [9,10], internal combustion engines [11,12], as well as in air conditioning systems as subsystems which provide processing (cooling) engine intake air or as autonomous systems in stationary [13–15] and transport application [16,17]. The various types of heat exchangers and feeding circuits are used for cooling air [18–20]. Combustion engines (gas turbines and internal combustion engines) are widely applied in power plants as primary driving engines [21–23] for power and heat generation (cogeneration plants) as well as gas engines [24,25] in combined cooling, heat and power plants [26,27] or integrated energy plants [28–30]. They found a wide application in stationary and transport energy plants. Fuel efficiency of gas turbines [31,32], diesel engines, and gas engines [33,34] decrease with increasing air temperature at the inlet [35,36].

A promising method for cooling the working fluid is to use a two-phase jet apparatus – a thermopressor [37,38]. In the thermopressor working (evaporation) chamber, the thermogasdynamic compression effect takes place, which consists of the following. When a highly dispersed liquid is injected into a gas (air) flow moving at a transonic velocity, instantaneous evaporation occurs with a simultaneous increase in the flow total pressure [39]. To ensure the highly efficient operation of the thermopressor, it is necessary to determine the technological requirements for the flow part design and the water-injected method in the apparatus. A significant influence on the working processes in the thermopressor is exerted by design factors. Energy is expended to compensate for losses associated with friction and to overcome local resistances of the confuser and diffuser sections of the flow path. Pressure losses due to aerodynamic resistance in the thermopressor flow part are determined by the local resistance coefficients: confuser (nozzle) – ζ_c; evaporation chamber – ζ_{ch}; diffuser – ζ_d.

Fowle and others have investigated the thermopressor operation that was installed for cooling the gas turbine exhaust gases [40]. An experimental jet apparatus had the following characteristics: the length

was 7.5 m, flow velocity was 31 m/s, gas mass flow was up to 11.5 kg/s. The pressure losses through local and hydraulic resistance in different parts of the thermopressor were obtained, the total pressure resistance without water injection reached 14 %.

Additionally, it was shown that the positive effect gained due to thermo-gas-dynamic compression in the thermopressor is greater, and the friction loss is smaller. Losses due to friction according to the classical method of calculation are up to 5–8 % [41,42]. Therefore, a substantial portion of present research is dedicated to the development of a methodology for calculating pressure losses, affected by design parameters, with specific attention to the resistance of the thermopressor confuser and diffuser. Thus, a primary objective is to optimize the design of the thermopressor's flow section to maximize efficiency in gas-dynamic processes through minimizing pressure losses.

3. PROBLEM STATEMENT

The general and principal advantage of a thermopressor as a contact heat exchanger compared to surface heat apparatus is the minimum surface friction due to instantaneous evaporation of highly dispersed liquid in accelerated superheated gas flow inside shortened mixing evaporative chamber. However, this effect leads to minimum pressure losses and, furthermore, to small pressure increment in the thermopressor as the whole when rational geometric parameters of the whole flow part and, first of all, the confuser and diffuser provide minimum local resistance. Therefore, their rational designing needs experimentally verified correlation for determining the local resistance coefficients of confuser and diffuser and justified characteristics on the influence of geometric parameters, including the angles of tapering and expanding flow parts, on pressure losses to define their rational values.

Issuing from the problem mentioned above, the research methodology involves the analysis of hydrodynamic processes in the flow part of thermopressor by using CFD simulation software, ANSYS Fluent. In addition, the experimental data is also considered to explore the impact of geometric parameters and flow characteristics on local resistance of the confuser and diffuser focused to optimize thermopressor design parameters providing minimum pressure losses and effective their implementation in the processes of intercooling air in gas turbines and charge air cooling in internal combustion engines.

A hydrodynamic analysis of thermopressor models was performed by using CFD simulation software ANSYS Fluent [42–44] to determine design parameters at various air Mach numbers.

The experimental thermopressor was developed to study the hydrodynamic processes in thermopressor flow part to determine the rational geometrical and regime parameters providing minimum pressure losses in operation conditions, corresponding to the cycle air parameters of gas turbines and charge air of internal combustion engines.

3. RESEARCH METHODOLOGY

A hydrodynamic analysis of typical models was carried out by using CFD simulation software ANSYS Fluent [42–44] to determine design parameters of the thermopressor (Fig. 1) at various air mass flow (M = 0.4–0.8).

The experimental thermopressor was developed to study the working processes in order to determine the rational geometrical and regime parameters. The initial parameters were following: pressure P_{tp1} and temperature T_{tp1}, corresponding to the cycle air parameters of gas turbines and charge air of internal combustion engines.

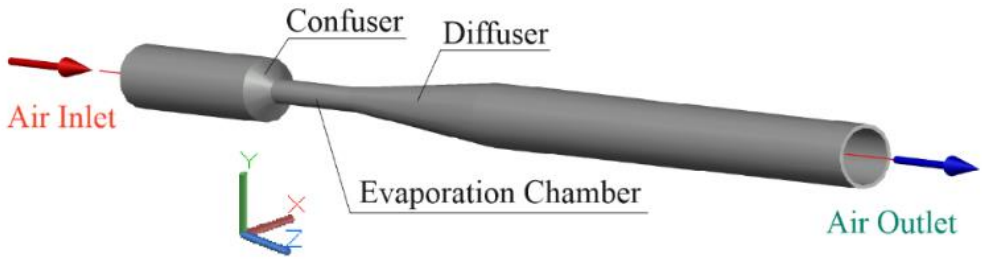

Figure 1. 3D thermopressor model.

The hydrodynamic processes numerical modeling is implemented in the ANSYS Fluent. In this case, the finite volume method was applied [45]. A calculation method was defined based on the Pressure-Based solvers, a turbulence model k-ε Realizable was used (this model is recommended for axisymmetric flows in jet devices) [46,47], and simulation results are processed and visualized with use of the appropriate functionality. The calculation of the airflow parameters (total pressure, dynamic pressure, velocity, temperature, turbulent kinetic energy, etc.) in the thermopressor was performed for several confuser and diffuser taper angles, as well as for several relative air velocity values in the evaporation chamber M = 0.4–0.8.

To determine the local resistance coefficients for the diffuser and confuser, classical methods of fluid flow mechanics [48,49] were used. The airflow was modeled as a stable, compressible, turbulent, and continuous flow. The turbulent flow model is based on a system of differential equations for the conservation of mass, momentum, and energy in the Eulerian formulation [50,51]. When modeling droplet trajectories, each individual droplet was tracked independently in the airflow by integrating the equations of motion, considering the influence of air resistance and gravity. The impact of turbulence on the droplets is investigated by computing the instantaneous air velocities in time-averaged Navier-Stokes equations [52,53] using a stochastic velocity model as part of the particle tracking model [54–58]. Additionally, the two-way coupling regime considered the influence of droplets on the airflow.

To check the adequacy of the obtained analytical dependencies for the local resistance coefficients, the experimental data were used [42].

It is suggested to use a thermopressor with an evaporator chamber diameter D_{ch} = 25 mm and an air flow rate through it of G_a = 0.29 kg/s (Table 1). The conicity angles of the converging nozzle (α_c = 30°) and the diverging nozzle (β_d = 5°) were chosen with the aim of minimizing losses to overcome frictional forces and local resistances in the narrowing-expanding sections of the device.

Table 1. Main geometric characteristics of the flow part of the thermopressor.

Parameter	**Value**
Length L_{tp}	387
Confusor (nozzle)	
Input diameter D_{c1}, mm	65
Output diameter D_{c2}, mm	25
The corner of the confusor α_c, °	30
The length L_c, мм (при α_c = 30 °)	34
Diffuser	
Input diameter D_{d1}, mm	25
Output diameter D_{d2}, mm	65
The corner of the diffuser β_d, °	5
Length L_d, мм (при β_d = 5 °)	228
Evaporation chamber (working chamber) at (L/D) = 5	
Diameter D_{ch}, mm	25
Length L_{ch}, mm	125

To ensure fine and uniform liquid dispersion in the thermopressor, a fine spray nozzle type can be employed. For such nozzles, the water dispersion at pressures above 3.5 MPa is in the range of δ_d = 20–30 μm. The nozzle placement should ensure an even distribution of droplets across the evaporator chamber's cross-section. In modelling the thermopressor, an assumption is made regarding droplet dispersion (spherical shape, droplet diameter of 3–30 μm) and the uniformity of their injection into the airflow. Thus, water spraying occurs at the beginning of the evaporator chamber, considering the even distribution of droplets across the chamber's cross-section (Fig. 2).

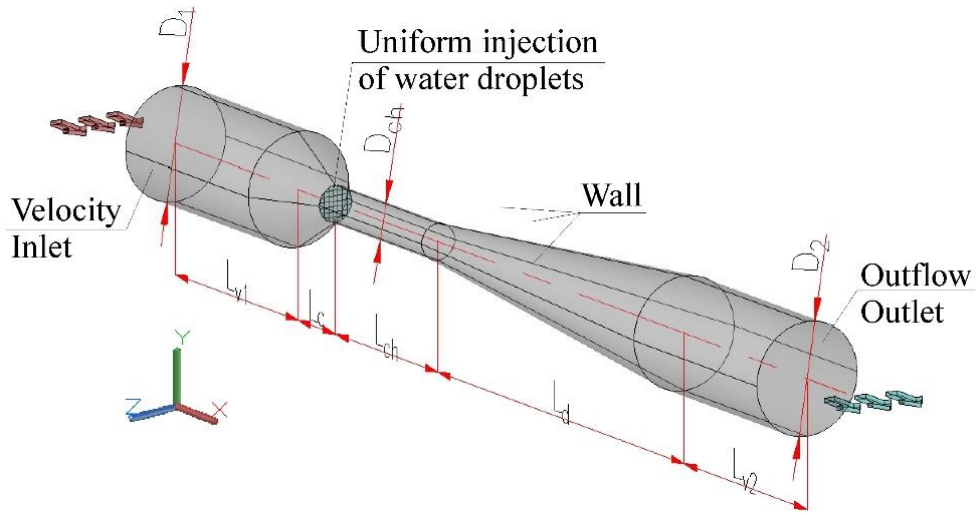

Figure 2. Calculated geometric model of the thermopressor.

The inlet and outlet sections of the geometric model are extended to eliminate the influence of edge effects in the computational model. The computational mesh (Fig. 3) is a hybrid mesh, with its primary elements constructed using an Automatic Method, and the mesh elements are tetrahedral. The boundary layer is constructed using Inflation, with prism elements, and wall layers specified in a quantity of 11 units.

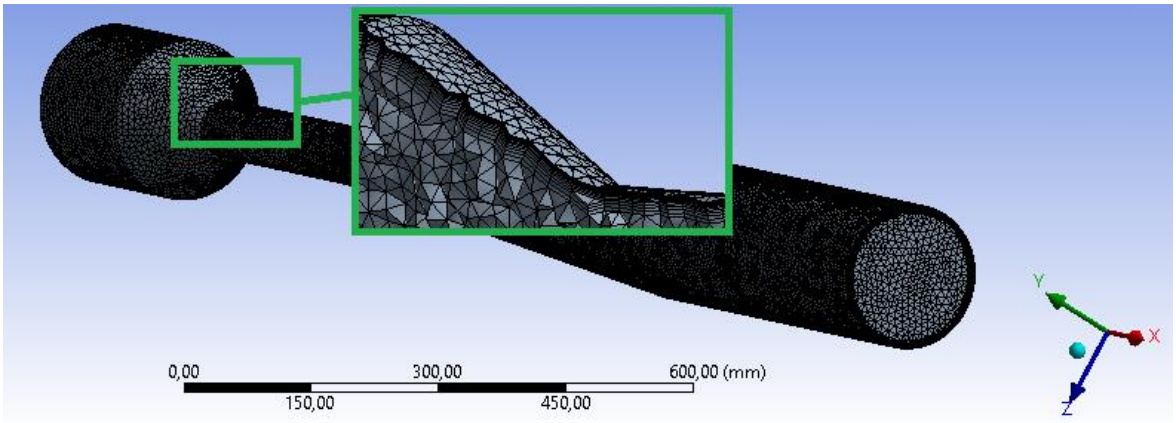

Figure 3. Calculation mesh for hydrodynamic modelling of the thermopressor.

The size of each mesh cell must be rational for effective computation and result consistency. Initially, a reliable solution was obtained for the continuous phase (without water injection), with a maximum size specified for each cell not exceeding 3 mm. The airflow at the inlet of the thermopressor is modelled with initial parameters of pressure, temperature, and relative humidity corresponding to the compressed air parameters after the first stage of the gas turbine compressor (Table 2).

Table 2. Technical characteristics of the experimental thermopressor model.

Parameter	Value
Air pressure at the inlet $P_{tp1}\cdot10^3$, Pa	301.3
Air temperature at the outlet T_{tp1}, K	473
Air speed at the outlet to the thermocompressor w_{a1}, m/s	40; 55
Mach number at the outlet to the mixing chamber M	0.45; 0.77
The relative velocity of the injected water (w_w/w_{a1})	0.33
The temperature of the water being injected T_{w1}, K	300
Mass flow of air G_a, kg/s	0.2–0.4
Relative mass flow rate of injected water g_w, %	5–11
The minimum diameter of sprayed water drops δ_{dmin}, μm	3
Maximum diameter of sprayed water drops δ_{dmax}, μm	30

Water droplets (discrete phase) are assumed to have a uniform spherical shape. Collisions and coalescence of droplets were not considered in the modelling due to the moderate concentration of water in the airflow (up to 11%) and the sufficiently rapid evaporation process. Droplet injection was conducted in the same direction as the flow, and the distribution of droplets in the injection plane was uniform. After colliding with the walls of the thermopressor, droplets reflect and continue moving in the airflow.

4. RESULTS AND DISCUSSIONS

According to the results of computer CFD modeling, the value of local resistance coefficients for the diffuser (divergent angle β = 6°; 8°; 10°; 12°) and confuser (convergent angle α = 30°; 35°; 40°; 45°; 50°) were determined. The initial parameters at the confuser inlet were following inlet pressure $P_{tp1} = 3\cdot10^5$ Pa; temperature T_{tp1} = 453 K, air velocity w_{air1} = 35 m/s. It should be noted that the nature of the change in velocity along the length of the thermopressor flow part was fairly uniform.

Basically, the local resistance coefficients, both for the confuser ζ_c and diffuser ζ_d, practically do not change at different velocity values M = 0.4–0.8 and Reynolds number Re. At the same time, the local resistance coefficient for confuser was – ζ_c = 0.02–0.08 (lower values correspond to the convergent angle α = 30 °). The influence of the diffuser resistance is more significant – ζ_d = 0.08–0.32 (lower values correspond to the divergent angle β = 6°). The absence of the Reynolds and Mach numbers influence on the local resistance coefficients indicates that there is a self-similar flow regime in the confuser and diffuser, which says that the coefficient of local resistance depends only on the flow channel geometry (convergent and divergent angle, expansion n_d and contraction n_c ratio) of the of the thermopressor.

The local resistance coefficient of the confuser ζ_c has been determined by following equation (the method of approximation depending on the geometric parameters was chosen):

$$\zeta_c = \sin\alpha\left(0.3287\sin\alpha - 0.2421\right) + n_c\left(7\cdot10^{-4}n_c - 0.0063\right) + 0.0858 \qquad (1)$$

This equation (regression coefficient – R = 0.9857; R^2 = 0.9715) has been obtained for the following flow characteristics of the confuser: Reynolds number was $1.2\cdot10^5 < Re < 3.4\cdot10^5$; convergent angle α = 30°–50°; Mach number M = 0.4–0.8; contraction ratio n_c = 5.6 – 8.5.

The deviation of the calculated values of the coefficient ζ_c from those obtained during numerical CFD modelling $\zeta_{e.c}$ is $\delta_c = (\zeta_{e.c} / \zeta_c)\cdot100\% = \pm 7$ % (Fig. 4).

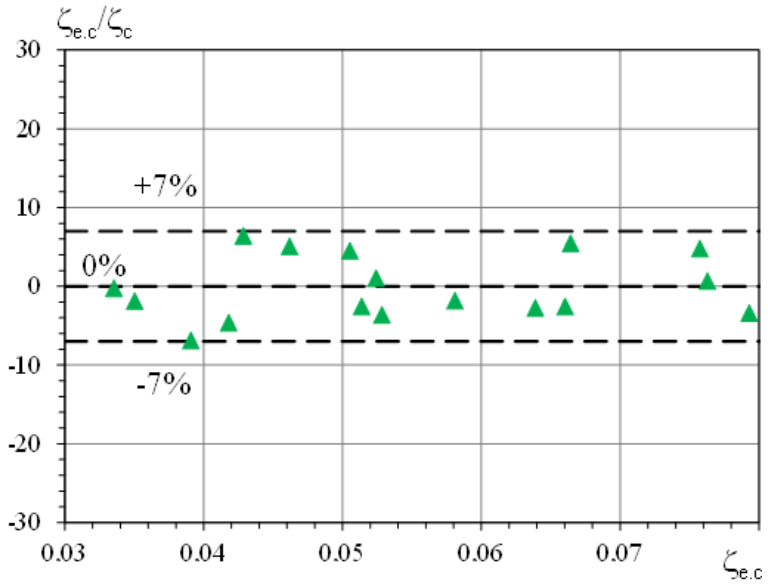

Figure 4. Comparison of the obtained local resistance coefficient for the confuser (ζc) with experimental data (ζe.c).

Determining the local resistance coefficient of the diffuser ζ_d is more difficult task due to the influence of interconnected geometric and operating parameters, the nature of the flow velocity field, and the boundary layer separation phenomenon. It must be pointed that the occurrence of the boundary layer separation takes place in almost all operation modes of the thermopressor. Thus, the supplementary disturbance of the air stream happens within the boundary layer in the diffuser at Mach number M above 0.4. This leads to the reverse air flow in the near-wall region that is caused by rising the flow tubulisation when the divergent angle of diffuser β is higher than 12° (Fig. 5). As a result, a flow separation occurs in the boundary layer, which, in turn, leads to a sharp increase in the local resistance coefficient ζ_d.

The local resistance coefficient of the diffuser ζ_d is determined by the following equation (the method of approximation depending on the geometric parameters was chosen):

$$\zeta_d = \sin\beta\left(0.428 + 6.4174\sin\beta\right) + n_d\left(0.0142 - 7\cdot10^{-4}n_d\right) - 0.0794 \qquad (2)$$

This equation (regression coefficient – R = 0.9828; R^2 = 0.9659) has been obtained for the following flow characteristics of the diffuser: Reynolds number was $1.2 \cdot 10^5 < Re < 3.4 \cdot 10^5$; divergent angle β = 4–12 °; Mach number M = 0.4–0.8; expansion ratio n_d = 4.4–8.7.

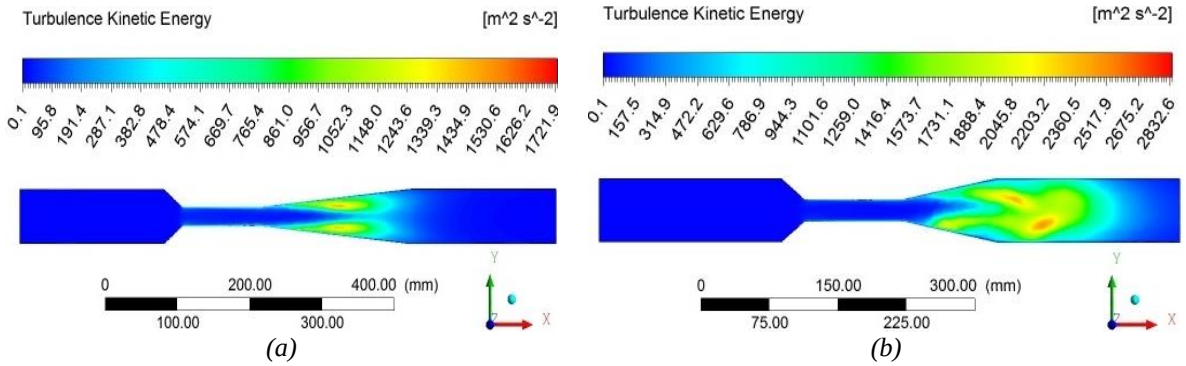

(a) *(b)*

Figure 5. Turbulent kinetic energy field distribution in the thermopressor flow part: at the diffuser divergent angle β = 6° (a) β = 12° (b) and Mach number M = 0.8

It should be noted that according to Fig. 4, the deviation of the calculated values of the coefficient ζ_c from those obtained during numerical CFD modelling $\zeta_{e.c}$ is $\delta_d = (\zeta_{e.c} / \zeta_c)$ 100% = ± 10%.

In addition, the similar comparison of the author theoretical values with the experimental results [42] were performed. As Fig. 7 shows, within the values of divergent angles β from 4° to 12° the diffuser local resistance coefficients calculated are within the acceptable error level of about 20%. At β = ≥ 12° (flow separation is present), the calculated values significantly exceed the experimental ones.

Analysis of the calculated data shows that the total pressure loss in a "dry" thermopressor (without liquid injection for evaporation) was ΔP_{loss} = 0.05–1.00·10^5 Pa (2–31%) at a fixed confuser convergent angle α = 40° and variable diffuser divergent angles β = 4–12 °. The total pressure loss was ΔP_{loss} = 0.05–0.40·10^5 Pa (1–12%) at a fixed diffuser divergent angle β = 6 ° and variable confuser convergent angles α = 30–50°. In this case, it is possible to recommend angles for the thermopressor flow parts (at the air mass flow G_{air} is up to 1 kg/s): confuser convergent angle α = 30° and diffuser divergent angle β = 4°, which correspond to the minimum pressure losses ΔP_{loss} = 1.0–9.5 %.

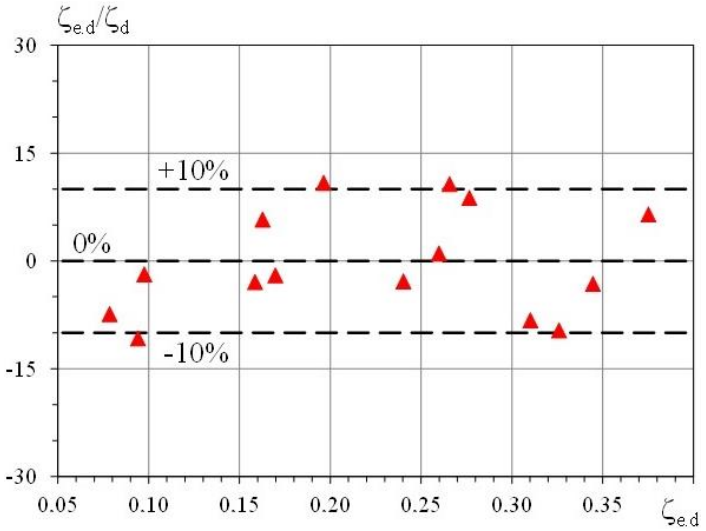

Figure 6. Comparison of the obtained local resistance coefficient for the diffuser (ζd) with experimental data (ζe.d)

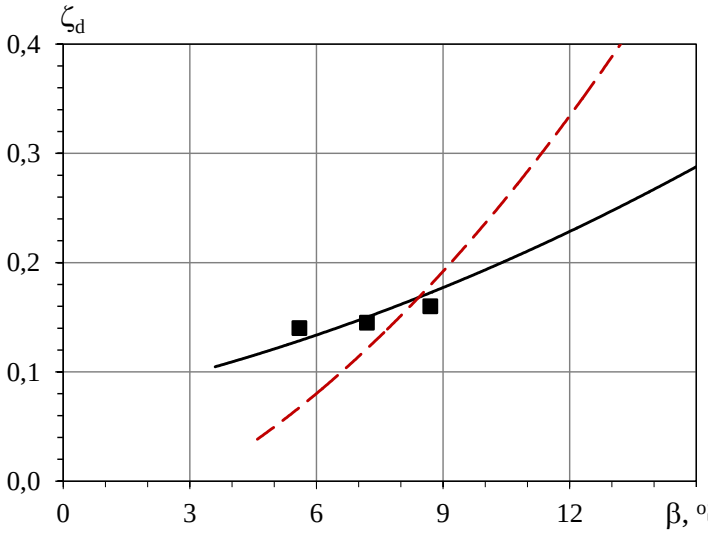

Figure 7. Comparison of the obtained local resistance coefficient for the diffuser (ζd) with the calculated ones depending on the divergent angle β: The calculated curve (dashed line) and experimental curve (full line) [42].

The Eqs. (1) and (2) might be applied for calculations of local resistance coefficient of the confuser and diffuser for similar hydrodynamic conditions of thermopressor operation. The confuser convergent angle α = 30 °and diffuser divergent angle β = 4 ° (at the air mass flow up to 1 kg/s), which provide the minimum pressure losses ΔP_{loss} = 1.0 – 9.5%, is recommended for designing thermopressors.

5. CONCLUSION

The research methodology involves the analysis of hydrodynamic processes in flow part of thermopressor by using CFD simulation software, ANSYS Fluent, and the experimental data to investigate the impact of geometric parameters and flow characteristics on local resistance of the confuser and diffuser to optimize thermopressor design parameters providing minimum pressure losses.

The equations for local resistance coefficients of confuser and diffuser, taking into account the Reynolds and Mach numbers and geometric angles, are received.

Determination of the main air flow parameters has been carried out for different channel geometry. The empirical equations for the local resistance coefficients of the confuser ζ_c and diffuser ζ_d of the thermopressor (at the air mass flow G_{air} up to 1 kg/s), taking into account the Reynolds and Mach numbers and geometric angles, have been determined. The equations have been obtained for the following flow characteristics: Reynolds number within $1.2 \cdot 10^5 < Re < 3.4 \cdot 10^5$; divergent angle $\beta = 4–12$ °; convergent angle $\alpha = 30°–50°$; Mach number $M = 0.4–0.8$; contraction ratio $n_c = 5.6–8.5$; expansion ratio $n_d = 4.4–8.7$.

The local resistance coefficients, determined by using computer CFD modeling, can be applied in designing practice: local resistance coefficients for confuser $\zeta_c = 0.02–0.08$ and diffuser $\zeta_d = 0.08 – 0.32$. The angles for tapering and expanding flow parts, which provide their minimum pressure losses from 1.0 to 9.5 %, were recommended to enable efficient operation of thermopressor as contact heat exhangers.

The findings contribute to optimizing the thermopressors design to ensure their efficient application for intercooling air in gas turbines and charge air in internal combustion engines to enhance power output and fuel efficiency.

REFERENCES

[1] Yang, Z, Kornienko, V, Radchenko, M, Radchenko, A, Radchenko, R. Research of exhaust gas boiler heat exchange surfaces with reduced corrosion when water-fuel emulsion combustion. *Sustainability* 2022; 14: 11927, DOI: 10.3390/su141911927.

[2] Kornienko, V, Radchenko, R, Bohdal, T, Radchenko, M, Andreev, A. Thermal Characteristics of the Wet Pollution Layer on Condensing Heating Surfaces of Exhaust Gas Boilers. In: Ivanov V, Pavlenko I, Liaposhchenko O, Machado J, Edl M, editors. Lecture Notes in Mechanical Engineering, Advances in Design, Simulation and Manufacturing IV, Proceedings of the 4th International Conference on Design, Simulation, Manufacturing: The Innovation Exchange, DSMIE-2021, Lviv, Ukraine, 8–11 June 2021; Springer: Cham, Switzerland, 2021; 2, pp. 339–348. DOI:10.1007/978-3-030-77823-1_34

[3] Yang, Z, Kornienko, V, Radchenko, M, Radchenko, A, Radchenko, R, Pavlenko, A. Capture of pollutants from exhaust gases by low-temperature heating surfaces. *Energies* 2022; *15*(1): 120. DOI:10.3390/EN15010120.

[4] Kornienko, V, Radchenko, R, Radchenko, M, Radchenko, A, Pavlenko, A, Konovalov, D. Cooling cyclic air of marine engine with water-fuel emulsion combustion by exhaust heat recovery chiller. *Energies* 2022; *15*: 248, DOI:10.3390/en15010248.

[5] Kurt, E, Demirci, M, Şahin, HM. Numerical analyses of the concentrated solar receiver pipes with superheated steam. Proceedings of the Institution of Mechanical Engineers, Part A: Journal of Power and Energy. 2022;236(5):893-910. doi:10.1177/09576509221074524.

[6] Radchenko, R, Tsoy, A, Forduy S, Anatoliy Z, Kalinichenko I. Utilizing the heat of gas module by an absorption lithium-bromide chiller with an ejector booster stage. In: *AIP Conference Proceedings 2020, Coimbatore, India, 17–18 July 2020;* AIP Publishing LLC: Melville, NY, USA, 2020; Volume 2285: 030084. DOI:10.1063/5.0026788.

[7] Radchenko, N, Trushliakov, E, Tsoy, A, Shchesiuk, O. Methods to determine a design cooling capacity of ambient air conditioning systems in climatic conditions of Ukraine and Kazakhstan. In: *AIP*

Conference Proceedings 2020, Coimbatore, India, 17–18 July 2020; AIP Publishing LLC: Melville, NY, USA, 2020; Volume 2285: 030074, DOI:10.1063/5.0026790.

[8] Trushliakov, E, Radchenko, M, Radchenko, A, Kantor, S, Zongming, Y. Statistical approach to improve the efficiency of air conditioning system performance in changeable climatic conditions. In ICSAI 2018 5th International Conference on Systems and Informatics; 10-12 November 2018: Jiangsu, Nanjing, China, pp. 256–260. DOI:10.1109/ICSAI.2018.8599434.

[9] Radchenko A, Tsoy A, Portnoi B, Kantor S. Increasing the efficiency of gas turbine inlet air cooling in actual climatic conditions of Kazakhstan and Ukraine. In: *AIP Conference Proceedings 2020, Coimbatore, India, 17–18 July 2020;* AIP Publishing LLC: Melville, NY, USA, 2020; Volume 2285: 030071, DOI:10.1063/5.0026787.

[10] Radchenko, M, Mikielewicz, D, Andreev, A, Vanyeyev, S, Savenkov, O. Efficient Ship Engine Cyclic Air Cooling by Turboexpander Chiller for Tropical Climatic Conditions. In: Nechyporuk M, Pavlikov V, Kritskiy D, editors. Lecture Notes in Networks and Systems, Proceedings of the Conference on Integrated Computer Technologies in Mechanical Engineering–Synergetic Engineering, ICTM 2020, Kharkiv, Ukraine, 28–29 October 2021; Cham, Switzerland: Springer, 2021; 188: pp. 498–507.

[11] Yang, Z, Konovalov, D, Radchenko, M, Radchenko, R, Kobalava, H, Radchenko, A, Kornienko, V. Analysis of efficiency of thermopressor application for internal combustion engine. *Energies* 2022; *15*: 2250, DOI:10.3390/en15062250.

[12] Yang, Z, Radchenko, R, Radchenko, M, Radchenko, A, Kornienko, V. Cooling potential of ship engine intake air cooling and its realization on the route line. *Sustainability* 2022; *14*: 15058, DOI:10.3390/su142215058.

[13] Radchenko, M, Radchenko, A, Trushliakov, E, Pavlenko, AM, Radchenko, R. Advanced method of variable refrigerant flow (VRF) systems designing to forecast on site operation–Part 1: General approaches and criteria. *Energies* 2023; *16*: 1381, DOI:10.3390/en16031381

[14] Radchenko, M, Radchenko, A, Trushliakov, E, Koshlak, H, Radchenko, R. Advanced method of variable refrigerant flow (VRF) systems designing to forecast on site operation– Part 2: Phenomenological simulation to recuperate refrigeration energy. *Energies* 2023; *16*: 1922, DOI:10.3390/en16041922

[15] Radchenko, M, Radchenko, A, Trushliakov, E, Pavlenko, A, Radchenko, R. Advanced method of variable refrigerant flow (VRF) system design to forecast on site operation–Part 3: Optimal solutions to minimize sizes. *Energies* 2023; *16*: 2417. https://doi.org/10.3390/en16052417

[16] Radchenko, N, Tsoy, A, Mikielewicz, D, Kantor, S, Tkachenko, V. Improving the efficiency of railway conditioners in actual climatic conditions of operation. In: *AIP Conference Proceedings 2020, Coimbatore, India, 17–18 July 2020;* AIP Publishing LLC: Melville, NY, USA, 2020; Volume 2285: 030072, DOI:10.1063/5.0026789.

[17] Radchenko, A, Radchenko, M, Trushliakov, E, Kantor, S, Tkachenko, V. Statistical method to define rational heat loads on railway air conditioning system for changeable climatic conditions. In ICSAI 2018 5th International Conference on Systems and Informatics; 10-12 November 2018: Jiangsu, Nanjing, China, pp. 1294–1298, DOI:10.1109/ICSAI.2018.8599355.

[18] Radchenko, N. A concept of the design and operation of heat exchangers with change of phase. *Archives of Thermodynamics* 2004; *25*(4): 3–18.

[19] Kruzel, M, Bohdal, T, Dutkowski, K, Radchenko, M. The Effect of Microencapsulated PCM Slurry Coolant on the Efficiency of a Shell and Tube Heat Exchanger. *Energies* 2022; *15*: 5142, DOI: 10.3390/en15145142

[20] Radchenko, NI. On reducing the size of liquid separators for injector circulation plate freezers. International Journal of Refrigeration 1985, 8(5), 267–269.

[21] Yang, Z, Radchenko, M. Radchenko, A, Mikielewicz, D, Radchenko, R. Gas turbine intake air hybrid cooling systems and a new approach to their rational designing. *Energies* 2022; *15*: 1474, DOI:10.3390/en15041474.

[22] Serbin, S, Radchenko, M, Pavlenko, A, Burunsuz, K, Radchenko, A, Chen, D. Improving Ecological Efficiency of Gas Turbine Power System by Combusting Hydrogen and Hydrogen-Natural Gas Mixtures. *Energies* 2023; *16*(9): 3618, DOI: 10.3390/en16093618

[23] Yu, Z, Shevchenko, S, Radchenko, M, Shevchenko, O, Radchenko, A. Methodology of Designing Sealing Systems for Highly Loaded Rotary Machines. *Sustainability* 2022; *14*(23): 15828, DOI:10.3390/su142315828.

[24] Radchenko, A, Scurtu, I-C, Radchenko, M, Forduy, S, Zubarev, A. Monitoring the efficiency of cooling air at the inlet of gas engine in integrated energy system. *Thermal Science* 2022, Part A; *26*(1): 185–194, DOI:10.2298/TSCI200711344R.

[25] Radchenko, A, Radchenko, M, Mikielewicz, D, Pavlenko, A, Radchenko, R, Forduy, S. Energy saving in trigeneration plant for food industries. *Energies* 2022; *15*: 1163, DOI:10.3390/en15031163.

[26] Forduy, S, Radchenko, A, Kuczynski, W, Zubarev, A, Konovalov, D. Enhancing the fuel efficiency of gas engines in integrated energy system by chilling cyclic air. In: Tonkonogyi V, Ivanov V, Trojanowska J, Oborskyi G, Edl M, Kuric I, Pavlenko I, Dasic P, editors. Lecture Notes in Mechanical Engineering, Advanced Manufacturing Processes, Selected Papers from the Grabchenko's International Conference on Advanced

Manufacturing Processes (InterPartner-2019), Odessa, Ukraine, 10–13 September 2019. Cham, Switzerland: Springer, 2020, pp. 500–509, DOI: 10.1007/978-3-030-40724-7_51.
[27] Radchenko, A, Radchenko, M, Koshlak, H, Radchenko, R, Forduy, S. Enhancing the efficiency of integrated energy system by redistribution of heat based of monitoring data. *Energies* 2022, *15*: 8774. DOI: 10.3390/en15228774
[28] Radchenko A, Radchenko M, Konovalov D, Zubarev A. Increasing electrical power output and fuel efficiency of gas engines in integrated energy system by absorption chiller scavenge air cooling on the base of monitoring data treatment. HTRSE-2018, E3S Web of Conferences 70, 6 p., 03011. DOI: 10.1051/e3sconf/20187003011.
[29] Radchenko, A, Mikielewicz, D, Forduy, S, Radchenko, M, Zubarev, A. Monitoring the Fuel Efficiency of Gas Engine in Integrated Energy System. In: Nechyporuk M, Pavlikov V, Kritskiy D, editors. Integrated Computer Technologies in Mechanical Engineering ICTM 2019, Advances in Intelligent Systems and Computing 2020, 1113. Springer, Cham, pp. 361–370. DOI: 10.1007/978-3-030-37618-5_31.
[30] Radchenko, M, Radchenko, A, Mikielewicz, D, Radchenko, R, Andreev, A. A novel degree-hour method for rational design loading. *Proc. Inst. Mech. Eng. Part A: Journal of Power and Energy* 2022; *237*(3): 570-579DOI:10.1177/09576509221135659.
[31] Konovalov, D, Tolstorebrov, I, Eikevik, TM, Kobalava, H, Radchenko, M, Hafner, A, Radchenko, A. Recent Developments in Cooling Systems and Cooling Management for Electric Motors. Energies 2023, 16, 7006, DOI: 10.3390/en16197006.
[32] Radchenko, M, Yang, Z, Pavlenko, A, Radchenko, A, Radchenko, R, Koshlak, H, Bao, G. Increasing the efficiency of turbine inlet air cooling in climatic conditions of China through rational designing—Part 1: A case study for subtropical climate: general approaches and criteria. *Energies* 2023; *16*: 6105, DOI: 10.3390/en16176105
[33] Radchenko, M., Radchenko, R., Kornienko, V., Pyrysunko, M. (2019) Semi-Empirical Correlations of Pollution Processes on the Condensation Surfaces of Exhaust Gas Boilers with Water-Fuel Emulsion Combustion. In: Ivanov, V., Pavlenko, I., Liaposhchenko, O., Machado, J., Edl, M. (eds) Advances in Design, Simulation and Manufacturing II. DSMIE 2019. Lecture Notes in Mechanical Engineering (LNME). Springer, Cham (2020), pp.853-862, 2020. Springer Nature Switzerland AG 2020. https://doi.org/10.1007/978-3-030-22365-6_85.
[34] Kornienko, V, Radchenko, M, Radchenko, A, Koshlak, H, Radchenko, R. Enhancing the Fuel Efficiency of Cogeneration Plants by Fuel Oil Afterburning in Exhaust Gas before Boilers. Energies 2023, 16, 6743, DOI: 10.3390/en16186743.
[35] Wang, K, Zhao, C, Cai, Y. Effect of intake air humidification and EGR on combustion and emission characteristics of marine diesel engine at advanced injection timing. *Journal of Thermal Science* 2021; *30*(4): 1174–1186.
[36] Danilecki, K, Eliasz, J. The Potential of Exhaust Waste Heat Use in a Turbocharged Diesel Engine for Charge Air Cooling. *SAE Technical Paper* 2020, pp. 2020–2089.
[37] Yang, Z, Korobko, V, Radchenko, M, Radchenko, R. Improving thermoacoustic low temperature heat recovery systems. *Sustainability* 2022; *14*: 12306. DOI: 10.3390/su141912306.
[38] Shapiro, AH, Wadleigh, KR. The aerothermopressor – a device for improving the performance of a gas-turbine power plant. Proceedings of the Trans. ASME, Cambridge, USA, 1956, pp. 617–653.
[39] Konovalov, D, Radchenko, M, Kobalava, H, Kornienko, V, Maksymov, V, Radchenko, A, Radchenko, R. Research of characteristics of the flow part of an aerothermopressor for gas turbine intercooling air. *Proceedings of the Institution of Mechanical Engineers, Part A: Journal of Power and Energy* 2022; *236*(4): 634-646. DOI: 10.1177/09576509211057952.
[40] Fowle, A. An Experimental Investigation of an Aerothermopressor Having a Gas Flow Capacity of 25 Pounds per Second. Massachusetts Institute of Technology, USA, 1972.
[41] Yu, Z, Løvås, T, Konovalov, D, Trushliakov, E, Radchenko, M, Kobalava, H, Radchenko, R, Radchenko, A. Investigation of thermopressor with incomplete evaporation for gas turbine intercooling systems. *Energies* 2023; *16*: 20, DOI: 10.3390/en16010020
[42] Konovalov D, Kobalava H, Radchenko M, Sviridov V, Scurtu I.C. Optimal Sizing of the Evaporation Chamber in the Low-Flow Aerothermopressor for a Combustion Engine. In: Tonkonogyi V, Ivanov V, Trojanowska J, Oborskyi G, Edl M, Kuric I, Pavlenko I, Dasic P, editors. Lecture Notes in Mechanical Engineering, Advanced Manufacturing Processes II (InterPartner 2020). Cham, Switzerland: Springer International Publishing, 2021. pp. 654–663.
[43] Fluent Tutorial Theory Guide Release 17.0. ANSYS, Inc. Canonsburg, 2016.
[44] Anderson, D, Tannehill, JC, Pletcher, RH. Computational Fluid Mechanics and Heat Transfer, third edition, 2016.
[45] Mazumder, S. Numerical Methods for Partial Differential Equations: Finite Difference and Finite Volume Methods, 2015.

[46] Zhou, Y. Rayleigh–Taylor and Richtmyer–Meshkov instability induced flow, turbulence, and mixing. *II. Physics Reports* 2017; 723–725: 1–160, DOI: 10.1016/j.physrep.
[47] Sirignano, WA. Fluid Dynamics and Transport of Droplets and Sprays. 2nd edn. New York: Cambridge University Press, 2010.
[48] Konovalov, D, Trushliakov, E, Radchenko, M, Kobalava, H, Maksymov, V. Research of the aerothermopresor cooling system of charge air of a marine internal combustion engine under variable climatic conditions of operation., In: Tonkonogyi V, Ivanov V, Trojanowska J, Oborskyi G, Edl M, Kuric I, Pavlenko I, Dasic P, editors. Lecture Notes in Mechanical Engineering, Advanced Manufacturing Processes, Selected Papers from the Grabchenko's International Conference on Advanced Manufacturing Processes (InterPartner-2019), Odessa, Ukraine, 10–13 September 2019. Cham, Switzerland: Springer, 2020, pp. 520–529, DOI: 10.1007/978-3-030-40724-7_53.
[49] Borghi, R, Anselmet, F. Turbulent Multiphase Flows with Heat and Mass transfer. Wiley-ISTE, 2013. ISBN: 978-1-848-21617-4.
[50] Duroudier, J. Fluid Transport: Pipes. 2016.
[51] Dixon, SL, Hall, CA. Fluid Mechanics and Thermodynamics of Turbomachinery. Elsevier Science, 7th edition. 2013.
[52] Schobeiri, MT. Turbomachinery Flow Physics and Dynamic Performance. 2012.
[53] Childs, P. Mechanical Design Engineering Handbook. 2018.
[54] Cumo, M, Naviglio A. Thermal Hydraulics. 2018.
[55] Granet, I, Bluestein, M. Thermodynamics and Heat Power: 9th edition. 2014.
[56] Deich, ME, Zaryankin AE. Gas Dynamics of Diffusers and Outlet Pipes of Turbomachines, Energy, 1970.
[57] Smith IK. The Supersonic Aerothermopressor. Proceedings of the Institution of Mechanical Engineers. 1969;184(1):121-132. doi:10.1243/PIME_PROC_1969_184_014_02
[58] Shapiro, A.H.; Wadleigh, K.R.; Gavril, B.D.; Fowle, A.A. The Aerothermopressor – A Device for Improving the Performance of a Gas-Turbine Power Plant. Trans. Am. Soc. Mech. Eng. 2022, 78, 617–650. https://doi.org/10.1115/1.4013756.